

Original Research

Apical Rotation as an Early Indicator of Left Ventricular Systolic Dysfunction in Acute Anterior Myocardial Infarction: Experimental Study

SAVVAS TH. TOUMANIDIS, ANNA KALADARIDOU, DIMITRIOS BRAMOS, ELIAS SKALTSIOTES, JOHN N. AGRIOS, NIKOLAOS VASILADIOTIS, CONSTANTINOS PAMBOUCAS, GEORGE KOTTIS, SPYRIDON D. MOULOPOULOS

Department of Clinical Therapeutics, Medical School, National and Kapodistrian University of Athens, "Alexandra" Hospital, Athens, Greece

Key words:
Speckle tracking
echocardiography,
twist.

Introduction: The aim of this study was to determine whether left ventricular (LV) apical rotation assessed by speckle tracking echocardiography (STE) can predict global LV systolic dysfunction after acute anterior myocardial infarction (AMI).

Methods: STE analysis was applied to LV short-axis images at the basal and apical levels in 21 open-chest pigs, before and after left anterior descending coronary artery ligation. LV radial and circumferential strain and strain rate, apical and basal rotation, and LV torsion were recorded.

Results: LV apical rotation ($3.68 \pm 1.73^\circ$ pre-AMI vs. $2.19 \pm 1.64^\circ$ post-AMI, $p < 0.009$), peak systolic rotation rate, and radial and circumferential strain as well as strain rate decreased significantly 30 min post-AMI. The LV global torsion decreased significantly. Strain and rotational changes of the LV apex were primarily correlated with ejection fraction (EF), but those of the LV base were not. EF had a significant correlation with the global LV twist ($r = 0.31$, $p < 0.05$). On multivariate linear regression analysis, fractional shortening of the long-axis (FSL) ($b = 0.58$, $p < 0.001$), rotation of the LV apex ($b = 0.32$, $p < 0.006$) and LV dp/dtmax ($b = 0.26$, $p < 0.02$) were independently related with EF. On analysis, of the receiver operating characteristic curve, the area under the curve for apical rotation was 0.765, $p < 0.006$; the best cutoff value of 2.92° had sensitivity 80% and specificity 71% in predicting $EF < 40\%$.

Conclusion: Apical rotation assessed by STE is a potential noninvasive early indicator of global LV systolic dysfunction in AMI and has a satisfactory association with LVEF. Its assessment could be valuable in clinical and research cardiology.

Manuscript received:
February 5, 2012;
Accepted:
September 10, 2012.

Address:
Savvas Toumanidis

80 Vas. Sophias Ave. &
Lourou
115 28 Athens, Greece
e-mail: stouman@otenet.gr

The complex architecture of left ventricular (LV) myocardial fibers is a vital contributor to normal LV performance.¹ Contraction of obliquely oriented myocardial fibers leads to a systolic wringing motion of the LV as a result of the opposing rotation of apex and base. Speckle tracking (STE) is a simple echocardiographic method for assessing LV strain, rotation and twist.² Previous studies (mainly clinical) evaluated LV twist and untwisting rate in patients with acute myocardial infarction (AMI), but

the acute impact of AMI on LV rotational/torsional mechanics and strain has not been adequately evaluated. Based on the earlier studies, the effect of AMI on LV systolic torsion appears to be related to the size rather than the site of the infarct, while global systolic torsion is independently correlated with LV ejection fraction (EF).³⁻⁵ Another experimental study demonstrated that radial and circumferential strains and torsion decreased significantly in the left anterior descending coronary artery (LAD) territory after its oc-

clusion.⁶ The assessment of the changes of LV geometry and function during the remodeling process after AMI is very important for prognosis and therapy, especially when investigating the impact of various treatment strategies.⁷⁻⁹ The aim of the present study was to investigate experimentally the value of LV apical rotation as an early indicator of LV global systolic dysfunction in acute AMI.

Methods

The protocol complied with the “Principles for the Care of Experimental Animals” and the “Guidelines for the Care and Use of Experimental Animals” issued by the US National Academy of Sciences and National Institute of Health (version 85-23, revision 1996) and was approved by the institutional animal research ethical review board of the “Alexandra” hospital.

Surgical preparation

Twenty-one healthy pigs, weighing 35 ± 5 kg, were sedated with an intramuscular administration of midazolam 5 mg/kg and ketamine potassium 5 mg/kg, anesthetized with intravenous (IV) thiopental sodium 5 mg/kg, intubated, and controlled by mechanical ventilation (Sulla 808V, Dräger Medizintechnik GmbH, Germany). Anesthesia was maintained with IV propofol 0.1-0.2 mg/kg. During the experiment, analgesia was maintained with the administration of opioid-fentanyl. Additional anesthetic was administered during the experiment as needed. A 7F sheath was inserted into the right internal jugular vein for the delivery of drugs and fluids. Fluid loss was compensated for by continuous infusion of saline into the right jugular vein. Through a left external carotid artery a 6F pigtail catheter was placed into the LV cavity and used for LV pressure monitoring. Lead II of the standard electrocardiogram (ECG), LV pressure, and hemoglobin oxygen saturation were monitored throughout the experiment. After catheter insertion, a 5000 IU heparin bolus was administered to avoid endovascular thrombus formation. The animal's temperature was monitored with a rectal thermometer. A suprapubic Foley catheter was placed. Vital signs and respiratory function were monitored to achieve homeostasis. Loading conditions were kept constant after AMI and/or during the different maneuvers.

A regular median sternotomy was performed

after thymic resection, a longitudinal pericardiectomy was performed and the LAD was surgically exposed. Two 3-0 Prolene (Ethicon, Johnson & Johnson Co., European Logistics Centre, Sint-Stevens-Woluwe, Belgium) sutures were placed after the origin of the first diagonal branch of the LAD, to be used for future ligation. The four ends of the two sutures were passed through an inflexible plastic tube 5 cm in length. While the ends of the sutures were secured, the tube was advanced toward the epicardium until its proximal part was 3-5 mm from the LAD. In this way, a suture loop tourniquet was created around the LAD, without ligation, ready for the next stage of the experiment. Before ligation, left coronary artery entrapment was confirmed by upward traction. The apex of the LV was observed for evidence of myocardial blanching indicating interruption in coronary flow, confirming epicardial ischemia.

Standard echocardiography

The echocardiographic study was performed using a Vivid *i* digital ultrasound system (GE Medical Systems Ultrasound Israel Ltd., Tirat Hacarmel, Israel) and a 3.5 MHz phased array transducer. Two-dimensional gray-scale echocardiographic images were obtained using 2nd harmonic imaging. Instrument settings were held constant for each experiment. The following parameters were measured before and 30 min after AMI:¹⁰ LV end-diastolic and end-systolic long- (Ld, Ls) and short-axis (Sd, Ss) dimensions, their fractional shortening (FSL%, FSS%), calculated by the formula: $FS (\%) = [(d-s)/d] \times 100$, the LV end-diastolic (EDV) and end-systolic (ESV) volumes, the EF (modified Simpson's rule). Stroke volume (SV) and cardiac output (CO) were measured and calculated from a subxiphoid epicardial apical four-chamber view. Mitral early (E) and late (A) diastolic flow velocities were measured and the mitral E/A ratio was calculated. The deceleration time of the mitral E wave was measured and tissue Doppler imaging of the lateral mitral annulus was obtained from the apical 4-chamber view. Systolic (S) and diastolic early (e') and late (a') mitral annulus velocities were measured. From these a diastolic e'/a' ratio was calculated. The ratio E/e' was also calculated. To determine the timing of cardiac events, mitral inflow and LV outflow were recorded using pulsed Doppler echocardiography. Three consecutive cardiac cycles were stored in cine loop format for off-line analysis. Averaged values were calculated for each parameter.

Two-dimensional strain imaging

LV rotation and twist were assessed by acquisition of specific short-axis planes with internal landmarks: the basal plane was acquired at the level of the mitral valve leaflets while excluding the mitral annulus and the apical plane was acquired distally to the papillary muscles. Every effort was made to make the LV cross section as circular as possible. The frame rate range was 65-80 /s. In each phase, three consecutive cardiac cycles' cine-loop images were stored for offline analysis with a dedicated platform EchoPac PC (version 7.0, GE Medical Systems). The endocardial border of each short axis was manually traced. A region of interest (ROI) was then drawn to include the entire myocardial thickness; care was taken to avoid including pericardium in the ROI. The position of the ROI and its width could be readjusted manually when the tracking appeared to be poor, in order to achieve optimal tracking. The software algorithm then automatically segmented the LV short axis into six equidistant segments. Finally, the software automatically defined the ventricular centroid for the mid myocardial line on a frame-by-frame basis, and calculated the time-domain LV strain (radial and circumferential), rotation and rotational velocity for each segment in both short-axis planes. Regional strain curves were then analyzed, and peak radial strain and peak circumferential strain were measured for each segment at both planes. The averaged LV rotation and rotational velocity profile were used for the calculation of LV twist and twist rate. As viewed from the apex, counterclockwise rotation was expressed as a positive value, whereas a clockwise rotation was denoted as a negative value.¹¹ LV twist was defined as the net difference between apical and basal rotation in degrees (°). Because the degree of rotation for the same amount of LV torque increases as the distance from the mid ventricular level increases, LV twist is expected to vary with the distance between the planes at which basal and apical short-axis images are obtained. LV torsion (°/mm) was calculated as LV twist/Ld longitudinal length (measured between the locations of the base and apex of the LV in the end-diastolic phase).¹¹ The opposite rotation after LV twist was defined as LV untwist and the time derivative of LV untwist was designated as the LV untwisting rate (°/s). The following parameters were measured: 1) peak apical and basal rotations and rates; 2) peak LV twist, torsion, torsion

rate and peak LV untwisting rate; and 3) peak apical and basal systolic radial and circumferential strains and strain rates.

Experimental protocol

After completion of the surgical preparations, a steady-state period of 15 min was allowed. Data were obtained initially before ligation of the LAD (control) and then 30 min after ligation. The acute MI was produced by ligation of the LAD, as a result of pulling on the four ends of the two sutures. The ligation was placed in the same position in all animals. Two animals were excluded from the post-AMI analysis due to unsuccessful recovery from ventricular fibrillation immediately after LAD ligation.

Statistical analysis

Results are presented as mean \pm SD. Variables were compared between the 2 groups using the unpaired Student's t-test. Multivariate regression analysis (forward stepwise) was performed to determine the independent associations of EF. Only significant variables on univariate analysis were entered as covariates in the multivariate model. The diagnostic usefulness of functional variables was compared using receiver operating characteristic curves. The best cutoff value was defined as the point with the highest sum of sensitivity and specificity. Results were expressed as area under the curve or 95% confidence interval for this area. A p-value <0.05 was considered statistically significant. Data analysis was performed using SPSS 19.0 (SPSS, Inc., Chicago, Illinois).

Results

Hemodynamics and conventional echocardiography

Measurements made after the acute anterior MI revealed a significant increase in LV long-axis end-systolic dimension (from 59.16 ± 6.21 mm to 63.64 ± 7.35 mm, $p < 0.04$) and a decrease in FSL (from $10.62 \pm 4.54\%$ to $3.95 \pm 3.01\%$, $p < 0.001$), while short-axis dimensions and FSS did not change significantly (Table 1). ESV increased significantly, whereas SV, EF and CO decreased significantly ($p < 0.001$ for all) post-AMI. Tissue Doppler early diastolic velocity of the mitral annulus e' ($p < 0.002$) and the e'/a' ratio ($p < 0.02$) decreased significantly. LV systolic pressure

Table 1. Comparison of the hemodynamic and conventional echocardiographic variables before and after myocardial infarction (MI).

	Pre-MI (n=21)	Post-MI (n=19)	p
Ld (mm)	66.20 ± 6.04	66.22 ± 7.12	0.99
Ls (mm)	59.16 ± 6.21	63.64 ± 7.35	<0.04
FSL (%)	10.62 ± 4.54	3.95 ± 3.01	<0.001
Sd (mm)	25.73 ± 2.80	26.37 ± 3.75	0.54
Ss (mm)	16.89 ± 2.35	18.19 ± 4.24	0.23
FSS (%)	34.09 ± 7.85	31.26 ± 10.59	0.34
Ld/Sd ratio	2.61 ± 0.35	2.57 ± 0.50	0.78
Ls/Ss ratio	3.59 ± 0.67	3.75 ± 1.19	0.60
EDV (ml)	62.36 ± 10.32	62.44 ± 14.59	0.98
ESV (ml)	29.77 ± 6.22	41.07 ± 10.34	<0.001
SV (ml)	32.59 ± 5.72	21.37 ± 6.17	<0.001
EF (%)	52.43 ± 5.13	34.21 ± 6.44	<0.001
CO (ml/min)	3038.35 ± 644.62	2257.62 ± 675.06	<0.001
E wave (mm/s)	62.05 ± 15.64	51.68 ± 10.48	0.20
A wave (mm/s)	62.67 ± 15.68	62.47 ± 13.51	0.97
E/A ratio	1.04 ± 0.39	0.86 ± 0.20	0.07
DT (ms)	136.17 ± 23.17	124.01 ± 35.82	0.21
TDI - S (cm/s)	0.09 ± 0.04	0.07 ± 0.03	0.20
TDI - e' (cm/s)	0.09 ± 0.03	0.06 ± 0.02	<0.002
TDI - a' (cm/s)	0.10 ± 0.03	0.15 ± 0.15	0.18
e'/a' ratio	1.03 ± 0.61	0.52 ± 0.24	<0.02
E/e' ratio	8.24 ± 4.36	9.81 ± 4.64	0.28
Heart rate (beats/min)	94.01 ± 17.57	107.16 ± 17.46	<0.02
LV systolic pressure (mmHg)	94.82 ± 11.87	84.50 ± 11.07	<0.007
LV mean pressure (mmHg)	62.13 ± 8.46	55.34 ± 8.85	<0.02
LV systolic pressure X heart rate (mmHg.beats/min)	8900.58 ± 2034.26	9096.23 ± 2130.31	0.77
LV EDP (mmHg)	8.80 ± 2.82	10.55 ± 3.94	0.11
LV dp/dtmax (mmHg/s)	1.38 ± 0.31	1.18 ± 0.32	0.06
QRS duration (ms)	72.75 ± 7.49	69.46 ± 6.53	0.15

Values are mean ± sd. A-wave – mitral late filling velocity; CO – cardiac output; DT – deceleration time of E-wave; LV – left ventricular; EDV – LV end-diastolic volume; EF – LV-ejection fraction; ESV – LV end-systolic volume; E-wave – mitral early filling velocity; FSL – fractional shortening-long axis; FSS – fractional shortening-short axis; Ld – LV end-diastolic long-axis dimension; Ls – LV end-systolic long-axis dimension; LV EDP – LV end-diastolic pressure; Sd – LV end-diastolic short-axis dimension; Ss – LV end-systolic short-axis dimension; SV – LV-stroke volume; TDI-a' – late diastolic mitral annulus velocity; TDI-e' – early diastolic mitral annulus velocity; TDI-S – peak systolic mitral annulus velocity; TDI – tissue Doppler imaging.

decreased (pre-AMI 94.82 ± 11.87 mmHg vs. 84.50 ± 11.07 mmHg post-AMI, $p < 0.007$), but heart rate increased significantly ($p < 0.02$). Eccentricity indexes (Ld/Sd, Ls/Ss ratio) did not change significantly.

Deformation and rotational changes

LV apical strain and rotational parameters were those mainly affected by the anterior AMI (Table 2). Rotation ($3.68 \pm 1.73^\circ$ pre-AMI vs. $2.19 \pm 1.64^\circ$ post-AMI, $p < 0.009$), peak systolic rotation rate, and radial and circumferential strain as well as strain rate decreased significantly (Figure 1). Deformation and rotational variables of the LV base did not change significantly. The LV global torsion decreased significantly ($0.13 \pm 0.03^\circ/\text{mm}$ vs. $0.10 \pm 0.04^\circ/\text{mm}$,

$p < 0.05$) while twist, systolic twisting and untwisting rate did not change significantly.

Changes in EF in the overall study population were mainly and significantly correlated with the fractional shortening of the LV long-axis (FSL, $r = 0.72$, $p < 0.001$), and showed secondary correlations with the FSS ($r = 0.32$, $p < 0.04$), LV systolic pressure ($r = 0.48$, $p < 0.002$) and $\text{LVdp/dt}_{\text{max}}$ ($r = 0.36$, $p < 0.02$, Table 3). Strain and rotational changes of the LV apex were primarily correlated with EF, but not those of the LV base (Figure 2). EF had a weak but significant correlation with the global LV twist ($r = 0.31$, $p < 0.05$). On multivariable linear regression analysis FSL ($b = 0.58$, $p < 0.001$), rotation of the LV apex ($b = 0.32$, $p < 0.006$) and $\text{LV dp/dt}_{\text{max}}$ ($b = 0.26$, $p < 0.02$) were independently related with EF.

Table 2. The effect of acute anterior myocardial infarction on strain and rotational variables of the left ventricle.

	Pre-MI (n=21)	Post-MI (n=19)	p
LV torsion (°/mm)	0.13 ± 0.03	0.10 ± 0.04	<0.05
LV twist (°)	8.36 ± 2.32	6.96 ± 2.63	0.08
LV systolic torsion rate (°/s)	58.84 ± 16.82	51.60 ± 13.44	0.15
LV untwisting rate (°/s)	-79.36 ± 26.04	-70.33 ± 24.50	0.27
LV base:			
Rotation (°)	-5.34 ± 1.51	-5.59 ± 2.09	0.66
Peak systolic rotation rate (°/s)	-42.82 ± 16	-47.19 ± 17.86	0.42
Peak radial strain	41.3 ± 13.76	42.04 ± 13.81	0.87
Peak systolic radial strain rate (s ⁻¹)	1.83 ± 0.55	1.83 ± 0.47	0.99
Peak systolic circumferential strain	-12.30 ± 3.72	-13.04 ± 2.65	0.48
Peak systolic circumferential strain rate (s ⁻¹)	-0.81 ± 0.27	-0.83 ± 0.26	0.80
LV apex:			
Rotation (°)	3.68 ± 1.73	2.19 ± 1.64	<0.009
Peak systolic rotation rate (°/s)	29.96 ± 12.82	18.55 ± 18.69	<0.03
Peak radial strain	40.86 ± 12.21	19.34 ± 13.69	<0.001
Peak systolic radial strain rate (s ⁻¹)	1.77 ± 0.51	1.42 ± 0.51	<0.03
Peak systolic circumferential strain	-15.33 ± 4.74	-9.82 ± 4.20	<0.001
Peak systolic circumferential strain rate (s ⁻¹)	-1.07 ± 0.28	-0.60 ± 0.18	<0.001

Values are mean ± sd. MI – myocardial infarction; LV – left ventricular.

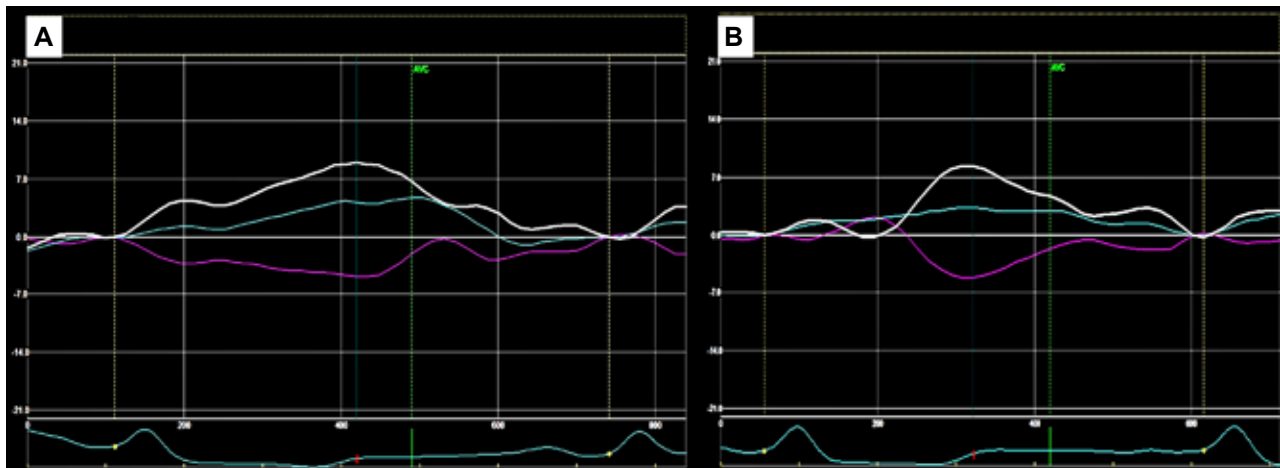


Figure 1. A. A representative case of left ventricular (LV) twist (8.94°) before acute myocardial infarction. The white color tracing denotes LV twist; blue denotes apical rotation (4.75°) and purple denotes basal rotation. AVC – aortic valve closure. B. The same animal 30 min post-AMI shows a minor reduction in LV twist (8.42°) and a significant reduction in apical rotation (3.23°).

On analysis of the receiver operating characteristic curve, the area under the curve for apical rotation was 0.765, $p < 0.006$; the best cutoff value of 2.92° had sensitivity 80% and specificity 71% for predicting $EF < 40\%$ (Figure 3).

Interobserver variabilities were $r = 0.90$ for EF and torsion (SE of estimation 8.8% and 8.6%, respectively). Intraobserver variabilities were $r = 0.95$ for EF and $r = 0.96$ for torsion (SE of estimation 4.3% and 5.4%, respectively).

Discussion

The present study provides new perspectives into the pathophysiology of the acute remodeling process 30 min after AMI. Myocardial cell necrosis after AMI results in an abnormal remodeling procedure, which typically alters LV size, geometry and function. Under the conditions of post-AMI remodeling, LV dilatation, interstitial fibrosis and scar tissue formation are considered responsible for LV torsional and dys-

Table 3. Significant correlations between ejection fraction and left ventricular function, deformation and rotational indices in the overall study population.

	Correlation coefficient with EF (%)	p<
FSL (%)	0.72	0.001
FSS (%)	0.32	0.04
DT (ms)	0.35	0.03
TDI-e' (cm/s)	0.46	0.003
LV systolic pressure (mmHg)	0.48	0.002
LV dp/dt _{max} (mmHg/s)	0.36	0.02
LV twist (°)	0.31	0.05
Apical rotation (°)	0.45	0.004
Apical peak systolic rotation rate (°/s)	0.46	0.003
Apical peak radial strain	0.51	0.001
Apical peak systolic circumferential strain	-0.37	0.02
Apical peak systolic circumferential strain rate (s ⁻¹)	-0.59	0.001

Abbreviations as in Table 1.

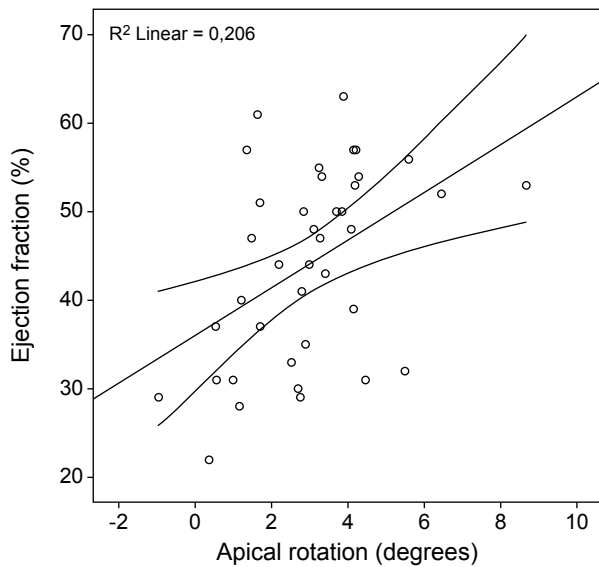


Figure 2. Correlation between left ventricular ejection fraction and apical rotation ($r=0.45$, $p<0.004$) as assessed by speckle-tracking echocardiography in the entire study population.

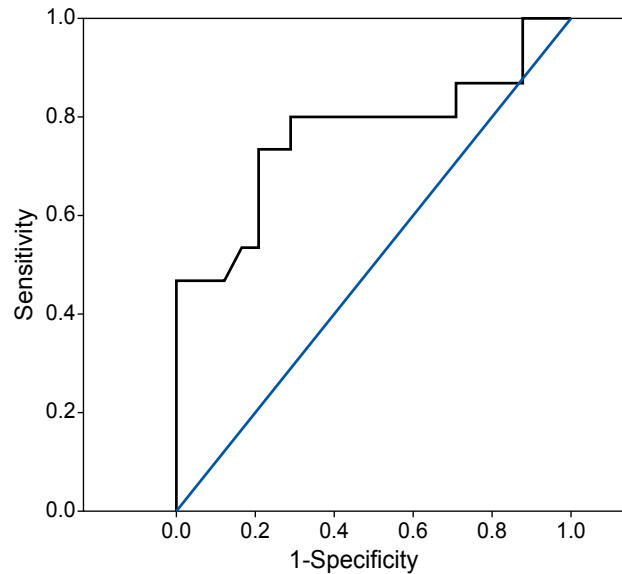


Figure 3. Receiver operating characteristic (ROC) curve, testing the accuracy of left ventricular (LV) apical rotation in the prediction of ejection fraction (EF) <40%. The best LV apical rotation cutoff value of 2.92° provided the highest sensitivity (80%) and specificity (71%) for predicting LVEF <40%. The area under the curve for apical rotation was 0.765 ($p<0.006$).

functional changes.^{13,14} This study demonstrates the value of apical rotation, reflecting the effect of acute myocardial cell necrosis on the strain and twisting properties of the myocardium, in predicting EF reduction before the development of typical post-AMI remodeling. It would be very difficult to carry out such a study in the clinical setting.

The main findings of this study can be summarized as follows:

1. There was an immediate decrease in the systolic

and diastolic performance of the myocardium, as depicted by the increase in the long-axis end-systolic dimension, the decrease in its fractional shortening, the increase in ESV, and the decrease in SV, EF, CO, e' and the e'/a' ratio.

2. LV apical strain and rotational properties were affected in the super-acute phase of the AMI, as depicted by the reduction of rotation, peak systolic rotation rate, radial and circumferential strain as well as strain rate.

- EF changes were correlated mainly with apical rotational and strain variables, while apical rotation was demonstrated to be an independent predictor of EF reduction.

Myocardial fiber orientation in the LV wall changes from a left-handed helix in the subepicardium to a right-handed helix in the subendocardium.¹⁵⁻¹⁸ Contraction of these obliquely oriented fibers creates a wringing or twisting motion of the LV. Torsional deformation is determined by the net effect of positive torsional deformation forces developing in the subepicardium and negative torsional deformation forces generated in the subendocardial fibers.¹⁶⁻¹⁸ The loss of torsion results from the diminution of counterclockwise apical rotation. These severe impairments of apical strain cannot generate sufficient apical rotational movement, which is the main determinant of LV systolic twist. This is a result of the reduction of circumferential strain in the apex, which may affect LV twist behavior. Our results show that rotation, peak systolic rotation rate, and radial and circumferential strain as well as strain rate were reduced significantly 30 min post LAD ligation.

Experimental^{18,19} and clinical²⁰ studies have demonstrated a decrease in LV rotation induced by acute ischemia. Animal models have suggested a marked reduction in rotational motion in transmural infarcts after coronary artery ligation.²¹ Several reports have confirmed a significant correlation between LV torsion and EF.^{4,22-24} However, the relative accuracy of apical LV rotation against EF under AMI has not been completely explored. Previous studies showed the pivotal role of apical rotation in assessing LV function in various heart diseases using tagged magnetic resonance imaging (MRI)²⁵⁻²⁷ or STE.^{3,11} A good agreement between MRI and STE for the assessment of the LV twist was validated in patients and controls.^{3,28-30} LV torsion is more influenced by apical rotation than by basal rotation, and apical rotation markedly decreases with AMI.¹¹ In a previous study, Kim et al proposed that apical rotation, assessed by STE, could be an effective noninvasive index of global LV contractility and was more closely related to dp/dt_{max} than LVEF.³¹ Our findings with multivariate analysis showed an independent association of LVEF with apical rotation, stronger than with dp/dt_{max} . LVEF is currently the most widely used index of LV systolic function. However, it should be noted that the development of wall motion abnormalities after AMI significantly decreases the accuracy

of LVEF. The inaccurate calculation in LV volume, despite the application of the biplane Simpson method, could explain the dramatic decrease of accuracy, because two-dimensional echocardiography depends on geometric assumptions and is subject to image-plane positioning errors. In contrast, apical rotation can be measured from parasternal short-axis views of the apex level, which have been routinely investigated for the detection of regional wall motion abnormalities. The fact that the decrease in LV apical rotation is observed irrespectively of coronary ligation or ligation sites suggests that apical rotation can serve as a marker of global, not local, LV function.^{19,31,32} Thus, LV apical rotation could provide a more accurate measurement of LV performance than does LVEF. Moreover, there was an immediate decrease in LV diastolic function after MI as depicted by the decrease in TDI indexes e' and the e'/a' ratio. A similar pattern was shown by the transmitral diastolic indexes E and E/A ratio, although the decrease was not statistically significant. The differences between transmitral and TDI indexes were probably due to the fact that TDI indexes are more sensitive markers of LV dysfunction.³³

Our results showed that apical and basal rotation responded differently to AMI. Apical rotation showed clear changes, whereas basal rotation exhibited no significant alterations. LVEF was correlated significantly with apical strain and rotational parameters, while correlations with basal parameters were non-significant. These results agree with those of previous studies.^{20,28}

These observations suggest that apical rotation can serve as a marker of LV contractility, and that its measurement using STE alone provides a noninvasive assessment of global LV function. If so, this technique is promising for use in routine clinical practice.

Limitations

There are some restrictions of the present acute study that limit the potential direct clinical implications. An important limitation is that experiments were performed in anesthetized open-chest pigs. Therefore, influences of anesthesia and open chest preparation on cardiac function and hemodynamics could not be excluded. The impairment of LV torsion observed early after AMI may be partially related to the presence of myocardial stunning; further studies are needed to assess the evolution of LV torsion after the acute phase of AMI.

Torsion assessment based on speckle tracking is highly dependent on image quality and frame rates, which are an inherent limitation. Low frame rates result in unstable speckle patterns, whereas high frame rates reduce scan-line density and reduce image resolution. However, previous studies have shown this to be of small magnitude and unlikely to affect torsion measurements significantly.³⁴ Technical developments in 3D speckle tracking with superior temporal and spatial resolution could theoretically circumvent the limitations of through-plane motion inherent in 2D imaging.

Longer-term animal studies are needed to determine if these early differences result in chronic ventricular remodeling. Any extrapolation of the data from the present study in pig hearts to patients with ischemic heart disease should be made with caution.

Clinical implications

The present study emphasizes the importance of LV apical rotation as a sensitive factor in LV systolic dysfunction. Its impairment early after AMI probably plays a significant role in the progress of LV remodeling. Consequently, this parameter could be used in clinical practice as an early sign for risk stratification. Early evaluation of LV apical rotation after AMI by STE may be able to identify patients with reduced apical rotation, who could benefit from aggressive medical therapy, revascularization and stem cell therapy, in order to avoid LV remodeling and cardiac failure. Although the clinical applications remain to be determined, STE is a widely available technique that enables the simple evaluation of LV torsion in humans.

References

1. Buckberg G, Hoffman JI, Mahajan A, Saleh S, Coghlan C. Cardiac mechanics revisited: the relationship of cardiac architecture to ventricular function. *Circulation*. 2008; 118: 2571-2587.
2. Geyer H, Caracciolo G, Abe H, et al. Assessment of myocardial mechanics using speckle tracking echocardiography: fundamentals and clinical applications. *J Am Soc Echocardiogr*. 2010; 23: 351-369.
3. Bansal M, Leano RL, Marwick TH. Clinical assessment of left ventricular systolic torsion: effects of myocardial infarction and ischemia. *J Am Soc Echocardiogr*. 2008; 21: 887-894.
4. Garot J, Pascal O, Diébold B, et al. Alterations of systolic left ventricular twist after acute myocardial infarction. *Am J Physiol Heart Circ Physiol*. 2002; 282: H357-362.
5. Nucifora G, Marsan NA, Bertini M, et al. Reduced left ventricular torsion early after myocardial infarction is related to left ventricular remodeling. *Circ Cardiovasc Imaging*. 2010; 3: 433-442.
6. Sun JP, Niu J, Chou D, et al. Alterations of regional myocardial function in a swine model of myocardial infarction assessed by echocardiographic 2-dimensional strain imaging. *J Am Soc Echocardiogr*. 2007; 20: 498-504.
7. Bertini M, Nucifora G, Marsan NA, et al. Left ventricular rotational mechanics in acute myocardial infarction and in chronic (ischemic and nonischemic) heart failure patients. *Am J Cardiol*. 2009; 103: 1506-1512.
8. Han W, Xie MX, Wang XF, et al. Assessment of left ventricular torsion in patients with anterior wall myocardial infarction before and after revascularization using speckle tracking imaging. *Chin Med J (Engl)*. 2008; 121: 1543-1548.
9. Saridakis NS, Toumanidis ST, Vintzileou AM, et al. Effect of dobutamine on left ventricular functional geometry after acute myocardial infarction: experimental study. *Hellenic J Cardiol*. 2007; 48: 72-79.
10. Lang RM, Bierig M, Devereux RB, et al. Recommendations for chamber quantification: a report from the American Society of Echocardiography's Guidelines and Standards Committee and the Chamber Quantification Writing Group, developed in conjunction with the European Association of Echocardiography, a branch of the European Society of Cardiology. *J Am Soc Echocardiogr*. 2005; 18: 1440-1463.
11. Takeuchi M, Nishikage T, Nakai H, Kokumai M, Otani S, Lang RM. The assessment of left ventricular twist in anterior wall myocardial infarction using two-dimensional speckle tracking imaging. *J Am Soc Echocardiogr*. 2007; 20: 36-44.
12. Rüssel IK, Götte MJ, Bronzwaer JG, Knaapen P, Paulus WJ, van Rossum AC. Left ventricular torsion: an expanding role in the analysis of myocardial dysfunction. *JACC Cardiovasc Imaging*. 2009; 2: 648-655.
13. Gaudron P, Eilles C, Kugler I, Ertl G. Progressive left ventricular dysfunction and remodeling after myocardial infarction. Potential mechanisms and early predictors. *Circulation*. 1993; 87: 755-763.
14. Bolognese L, Cerisano G. Early predictors of left ventricular remodeling after acute myocardial infarction. *Am Heart J*. 1999; 138: S79-83.
15. Hansen DE, Daughters GT 2nd, Alderman EL, Stinson EB, Baldwin JC, Miller DC. Effect of acute human cardiac allograft rejection on left ventricular systolic torsion and diastolic recoil measured by intramyocardial markers. *Circulation*. 1987; 76: 998-1008.
16. Ingels NB Jr, Hansen DE, Daughters GT 2nd, Stinson EB, Alderman EL, Miller DC. Relation between longitudinal, circumferential, and oblique shortening and torsional deformation in the left ventricle of the transplanted human heart. *Circ Res*. 1989; 64: 915-927.
17. Moon M, Ingels D, Stinson E, Hansen D, Miller D. Alterations in left ventricular twist mechanics with inotropic stimulation and volume loading in human subjects. *Circulation*. 1994; 89: 142-150.
18. Kroeker CA, Tyberg JV, Beyar R. Effects of ischemia on left ventricular apex rotation. An experimental study in anesthetized dogs. *Circulation*. 1995; 92: 3539-3548.
19. Buchalter MB, Rademakers FE, Weiss JL, Rogers WJ, Weisfeldt ML, Shapiro EP. Rotational deformation of the canine left ventricle measured by magnetic resonance tagging: effects of catecholamines, ischaemia, and pacing. *Cardiovasc Res*. 1994; 28: 629-635.

20. Nagel E, Stuber M, Lakatos M, Scheidegger MB, Boesiger P, Hess OM. Cardiac rotation and relaxation after anterolateral myocardial infarction. *Coron Artery Dis.* 2000; 11: 261-267.
21. Lima JAC, Ferrari VA, Reichek N, et al. Segmental motion and deformation of transmurally infarcted myocardium in acute postinfarct period. *Am J Physiol.* 1995; 268 (3 Pt 2): H1304-H1312.
22. Dong SJ, Hees PS, Huang WM, Buffer SA Jr, Weiss JL, Shapiro EP. Independent effects of preload, afterload, and contractility on left ventricular torsion. *Am J Physiol.* 1999; 277 (3 Pt 2): H1053-H1060.
23. Kim HK, Sohn DW, Lee SE, et al. Assessment of left ventricular rotation and torsion with two-dimensional speckle tracking echocardiography. *J Am Soc Echocardiogr.* 2007; 20: 45-53.
24. Mornos C, Ruşinaru D, Manolis AJ, Zacharopoulou I, Pittaras A, Ionac A. The value of a new speckle tracking index including left ventricular global longitudinal strain and torsion in patients with dilated cardiomyopathy. *Hellenic J Cardiol.* 2011; 52: 299-306.
25. Tibayan FA, Lai DT, Timek TA, et al. Alterations in left ventricular torsion in tachycardia-induced dilated cardiomyopathy. *J Thorac Cardiovasc Surg.* 2002; 124: 43-49.
26. Yun KL, Niczyporuk MA, Daughters GT 2nd, et al. Alterations in left ventricular diastolic twist mechanics during acute human cardiac allograft rejection. *Circulation.* 1991; 83: 962-973.
27. Nagel E, Stuber M, Burkhard B, et al. Cardiac rotation and relaxation in patients with aortic valve stenosis. *Eur Heart J.* 2000; 21: 582-589.
28. Helle-Valle T, Crosby J, Edvardsen T, et al. New noninvasive method for assessment of left ventricular rotation: speckle tracking echocardiography. *Circulation.* 2005; 112: 3149-3156.
29. Notomi Y, Setser RM, Shiota T, et al. Assessment of left ventricular torsional deformation by Doppler tissue imaging: validation study with tagged magnetic resonance imaging. *Circulation.* 2005; 111: 1141-1147.
30. Amundsen BH, Helle-Valle T, Edvardsen T, et al. Noninvasive myocardial strain measurement by speckle tracking echocardiography: validation against sonomicrometry and tagged magnetic resonance imaging. *J Am Coll Cardiol.* 2006; 47: 789-793.
31. Kim WJ, Lee BH, Kim YJ, et al. Apical rotation assessed by speckle-tracking echocardiography as an index of global left ventricular contractility. *Circ Cardiovasc Imaging.* 2009; 2: 123-131.
32. Knudtson ML, Galbraith PD, Hildebrand KL, Tyberg JV, Beyar R. Dynamics of left ventricular apex rotation during angioplasty: a sensitive index of ischemic dysfunction. *Circulation.* 1997; 96: 801-808.
33. Yu CM, Sanderson JE, Marwick TH, Oh JK. Tissue Doppler imaging a new prognosticator for cardiovascular diseases. *J Am Coll Cardiol.* 2007; 49: 1903-1914.
34. Notomi Y, Lysyansky P, Setser RM, et al. Measurement of ventricular torsion by two-dimensional ultrasound speckle tracking imaging. *J Am Coll Cardiol.* 2005; 45: 2034-2041.